Electronic Supplementary Material (ESI) for Journal of Materials Chemistry A.

Supplementary Information - Data-driven Selection of Electrolyte Additives for Aqueous Magnesium Batteries

Tim Würger,[†,‡] Linqian Wang,[†] Darya Snihirova,[†] Min Deng,[†] Sviatlana V. Lamaka,[†] David A. Winkler,[¶,§,‖] Daniel Höche,[†] Mikhail L. Zheludkevich,[†,⊥] Robert H. Meißner,[*,†,‡] and Christian Feiler[*,†]

†*Institute of Surface Science, Helmholtz-Zentrum Hereon, Geesthacht, Germany*

‡*Institute of Polymers and Composites, Hamburg University of Technology, Hamburg, Germany*

¶*School of Biochemistry and Genetics, Latrobe University, Bundoora, Australia*

§*Monash Institute of Pharmaceutical Sciences, Monash University, Parkville, Australia*

‖*School of Pharmacy, University of Nottingham, Nottingham, United Kingdom*

⊥*Institute for Materials Science, Faculty of Engineering, Kiel University, Kiel, Germany*

E-mail: robert.meissner@tuhh.de; christian.feiler@hereon.de

Contents

Abbreviations of Chemicals **3**

Hyperparameter Tuning **3**

Feature Selection **4**

Uncertainty Estimation **5**

Discharge Experiments **6**

Discussion on Experiments **9**

Comparison of Structure-Activity Landscapes **10**

References **11**

Abbreviations of Chemicals

Table S1: Abbreviations for a selection of chemicals used in the discharge experiments.

Abbreviation	IUPAC Name
ACES	2-[(2-amino-2-oxoethyl)amino]ethanesulfonic acid
BES	2-[bis(2-hydroxyethyl)amino]ethanesulfonic acid
CAPS	3-(cyclohexylamino)propane-1-sulfonic acid
CHES	2-(cyclohexylamino)ethanesulfonic acid
DTPA	2-[bis[2-[bis(carboxymethyl)amino]ethyl]amino]acetic acid
EDTA	2-[2-[bis(carboxymethyl)amino]ethyl-(carboxymethyl)amino]acetic acid
EGTA	2-[2-[2-[2-[bis(carboxymethyl)amino]ethoxy]ethoxy]ethyl-(carboxymethyl)amino]acetic acid
HEPES	2-[4-(2-hydroxyethyl)piperazin-1-yl]ethanesulfonic acid
MES	2-morpholin-4-ylethanesulfonic acid
MOPS	3-morpholin-4-ylpropane-1-sulfonic acid
NTA	2-[bis(carboxymethyl)amino]acetic acid
TAPSO	3-[[1,3-dihydroxy-2-(hydroxymethyl)propan-2-yl]amino]-2-hydroxypropane-1-sulfonic acid
TES	2-[[1,3-dihydroxy-2-(hydroxymethyl)propan-2-yl]amino]ethanesulfonic acid
TIRON	4,5-dihydroxybenzene-1,3-disulfonic acid

Hyperparameter Tuning

Table S2: Hyperparameter tuning results for the SOAP-based S-model and distinct descriptor-based D-model. Parameter definitions and their associated equations are based on Musil et al.[1] and Helfrecht et al.[2]

Parameter	S_K	D_K
cutoff radius r_c	8.0	–
Gaussian width ξ	0.3	–
power ζ	2.0	–
regularization parameter γ	0.05	0.30
mixing parameter α	0.5	0.5
number of features n	–	12

Feature Selection

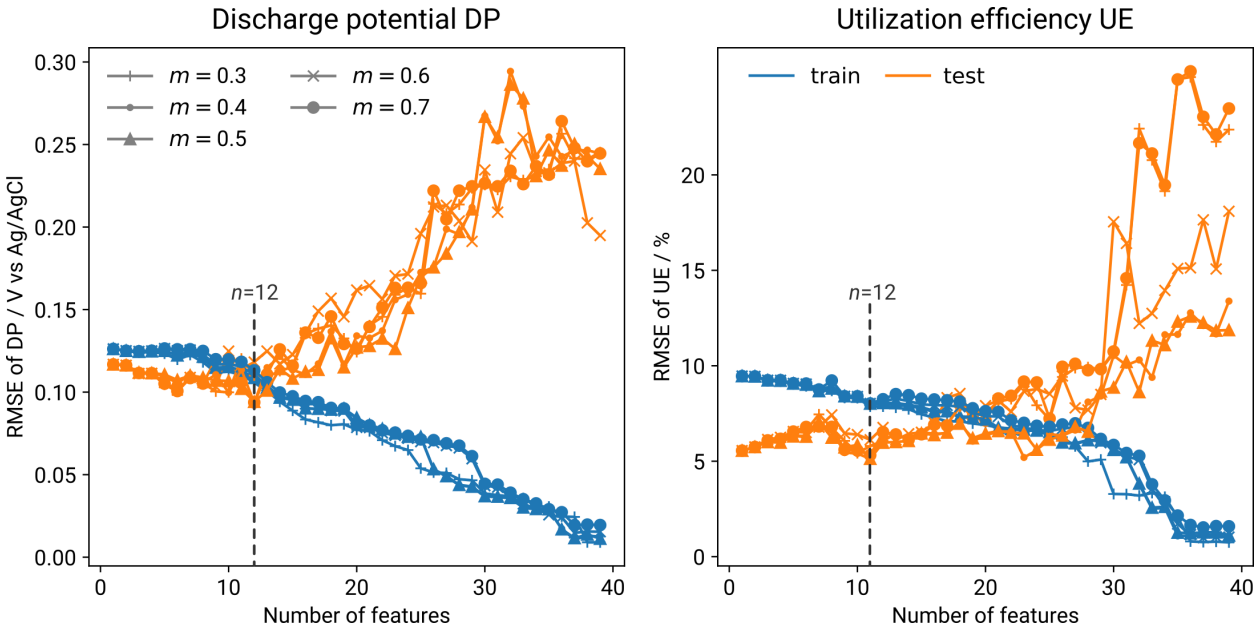

Figure S1: RMSE with respect to the number of features, as determined by CUR matrix decomposition and 5-fold cross validation. Results are shown for different mixing factors used to balance the KPCA and KRR components of the KPCovR model. Training and test errors are marked as blue and orange, respectively. Model training on 12 features leads to a minimal test error for DP and UE.

Uncertainty Estimation

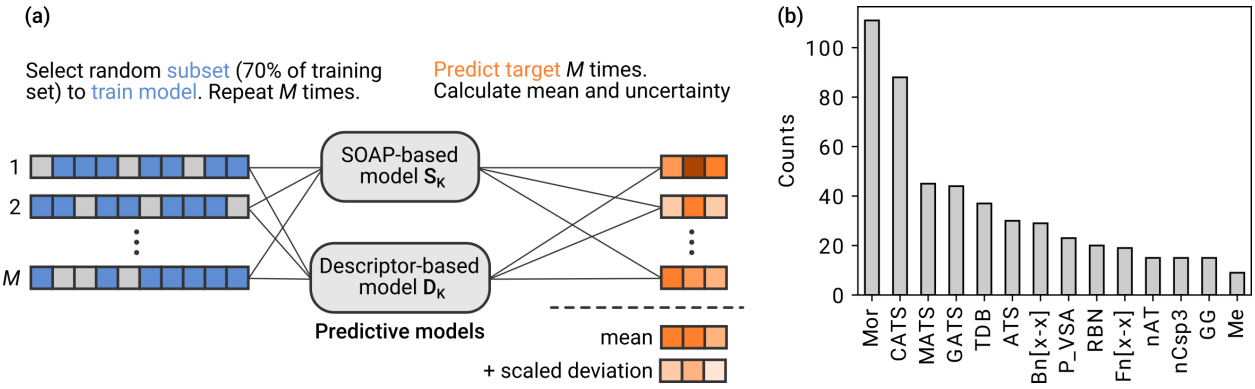

Figure S2: Uncertainty estimation for the predictions of S_K and D_K. (a) M random subsets are selected from the training dataset and used to train the same amount of M S-models and D-models. The target is predicted by the committee model, defined as the average of all M subset predictions. The single point uncertainty can be calculated and calibrated as described by Musil et al.[1,1] and Imbalzano et al.[3,3] (b) Distribution of features for $M = 50$ subset models during training of D_K. For each subset model, 12 features were selected by CUR matrix decomposition.

Discharge Experiments

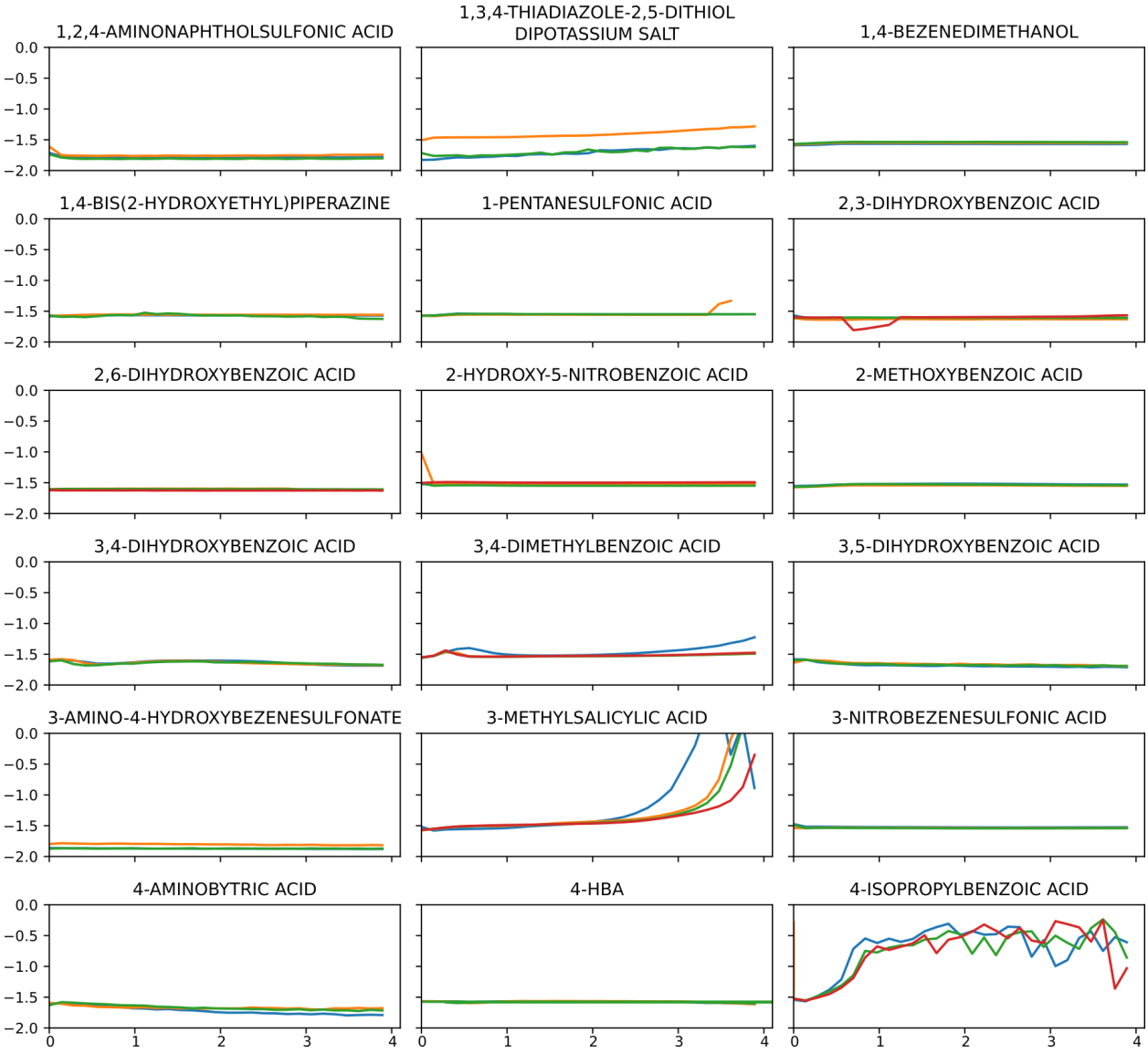

Figure S3: Discharge curves for the conduced discharge experiments. The x-axes show the time in hours, the y-axes the discharge potential in V vs. Ag/AgCl. Multiple colors indicate multiple runs of the same experiment. The fluctuations in the discharge behaviour can be attributed to the formation of surface films during discharge.

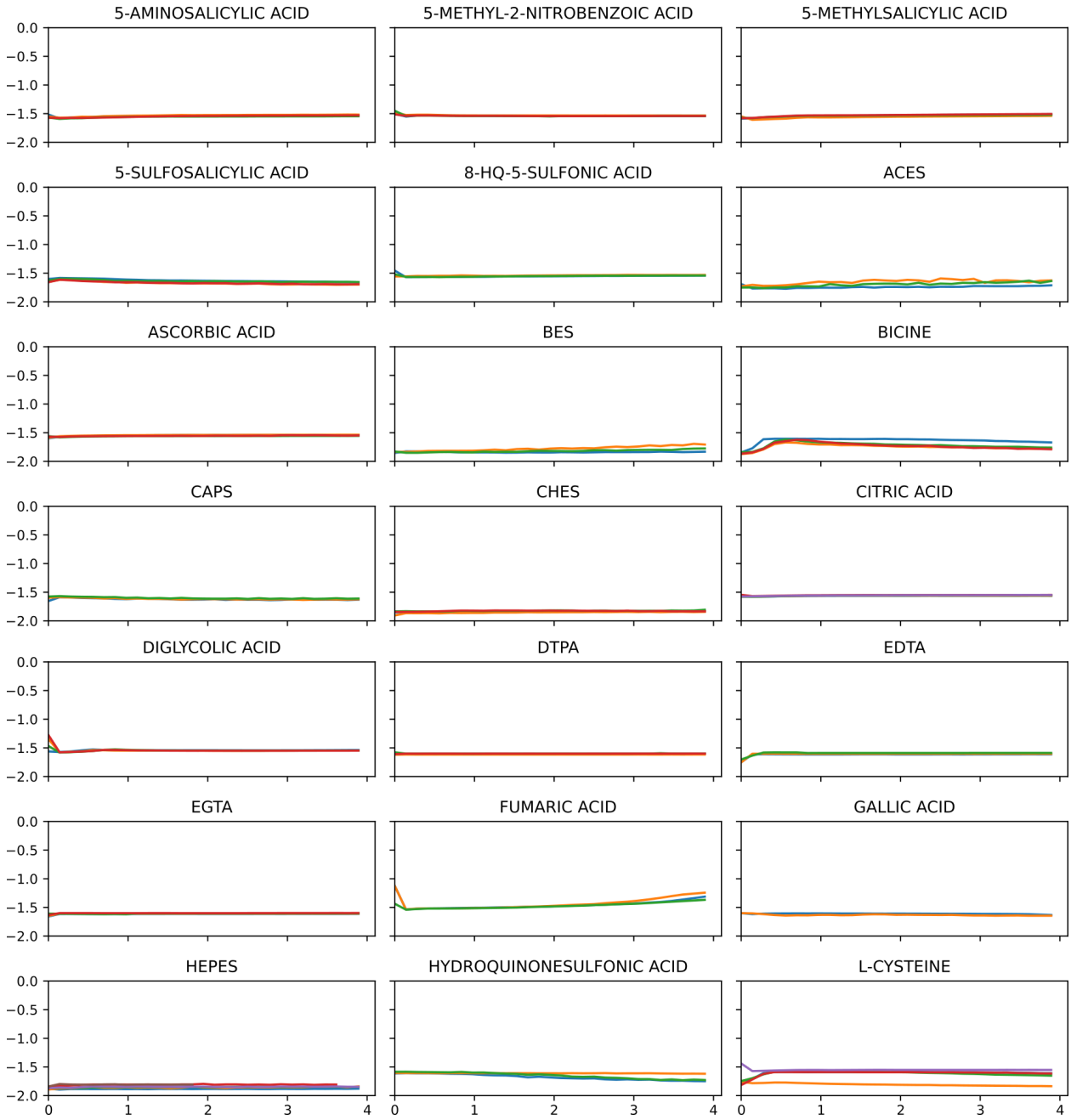

Figure S4: Discharge curves for the conduced discharge experiments. The x-axes show the time in hours, the y-axes the discharge potential in V vs. Ag/AgCl. Multiple colors indicate multiple runs of the same experiment.

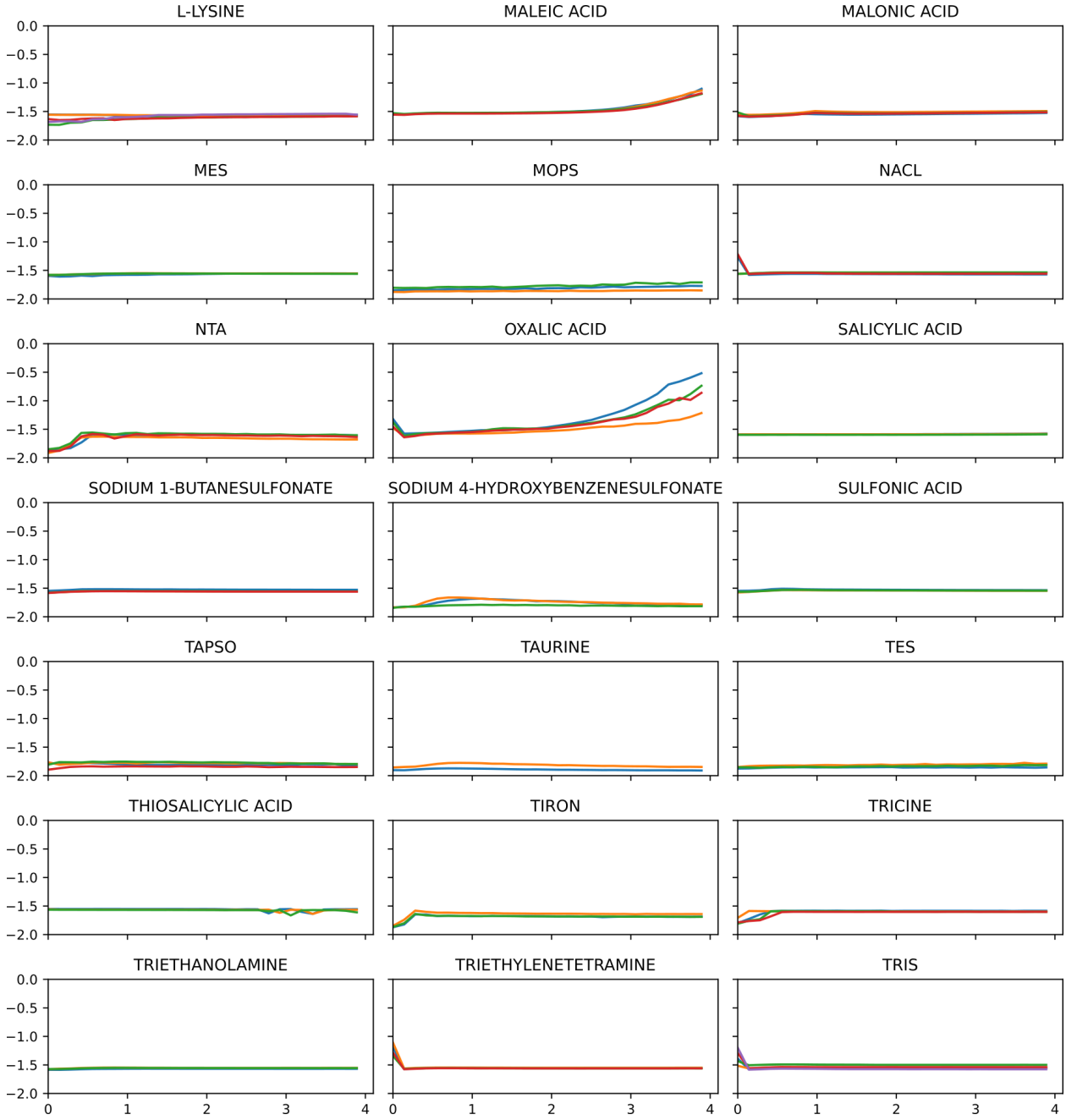

Figure S5: Discharge curves for the conduced discharge experiments. The x-axes show the time in hours, the y-axes the discharge potential in V vs. Ag/AgCl. Multiple colors indicate multiple runs of the same experiment.

Discussion on Experiments

In the experiment, compound II.1 (4-isopropylbenzoic acid) showed unusual discharge behavior, resulting in an abnormal discharge potential (DP). The results from three parallel discharge tests are shown in Figure S6.

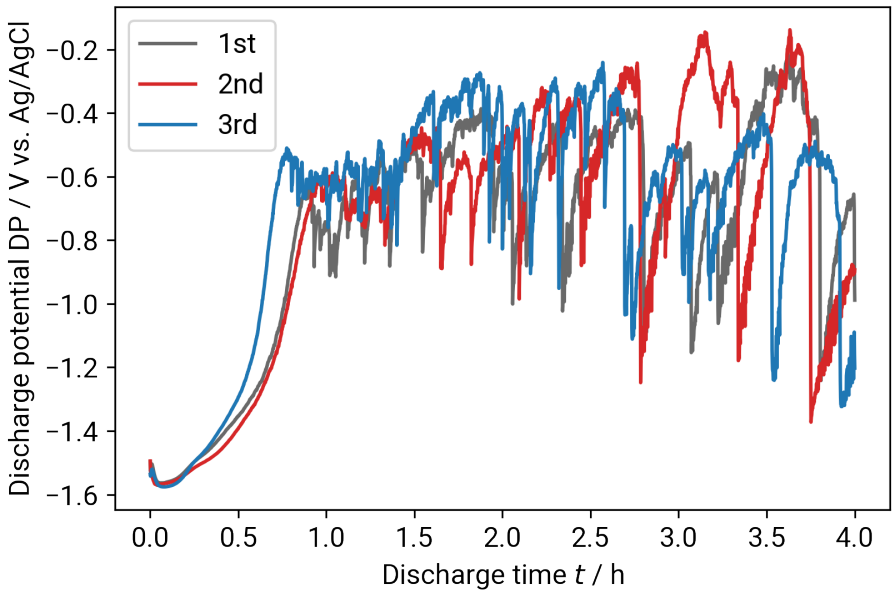

Figure S6: Discharge curves for compound II.1 (4-isopropylbenzoic acid).

The DP of a Mg-0.15Ca anode in 4-isopropylbenzoate-containing electrolyte continuously jumps between -1.2 and -0.2 V vs. Ag/AgCl. 4-isopropylbenzoate is reported as an efficient corrosion inhibitor for pure Mg and AZ-series Mg alloys.[4] It is very likely that the gradual positive shift of discharge potential is caused by the formation of a passive and dense deposit layer on the electrode surface. The sudden negative shift of discharge potential is due to the self-peeling of this deposit layer after the accumulation of discharge products on the electrode surface. During the experiment, layer formation (voltage drop) and self-peeling (voltage rise) alternate, leading to the observed discharge behavior.

Comparison of Structure-Activity Landscapes

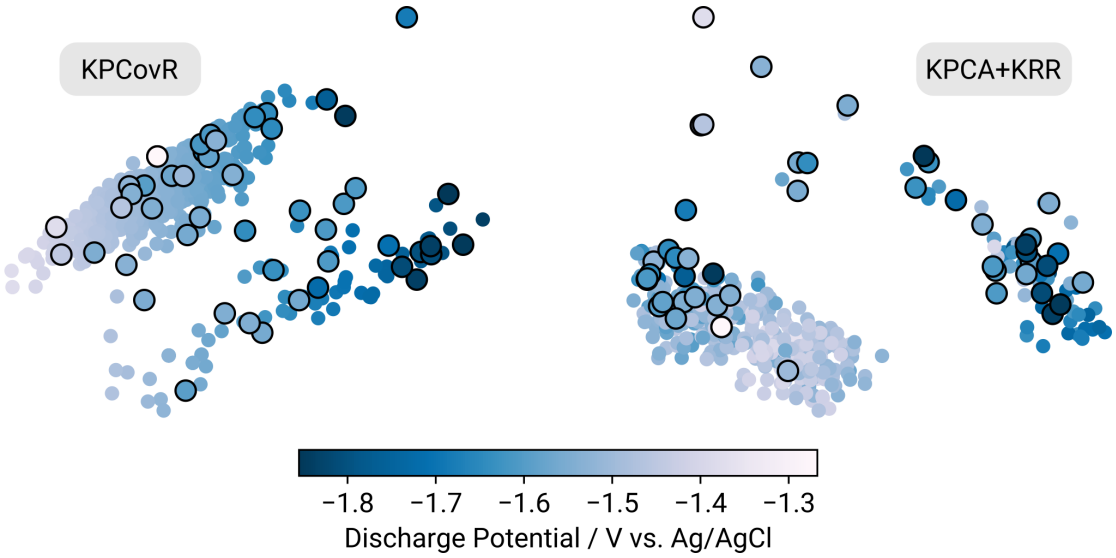

Figure S7: Structure-activity landscapes as derived from a SOAP kernel determined for 49 battery additives (black-rimmed dots) and 491 chemical compounds of a commercial database. In contrast to a combination of kernel principal component analysis (KPCA) and kernel ridge regression (KRR), similarity maps derived from kernel principal covariates regression (KPCovR) already incorporate the target property (here DP) in the two-dimensional projection. Hence, interpretations of underlying structure-activity relationships are facilitated and more intuitive.

References

(1) Musil, F.; De, S.; Yang, J.; Campbell, J. E.; Day, G. M.; Ceriotti, M. Machine learning for the structure-energy-property landscapes of molecular crystals. *Chemical Science* **2018**, *9*, 1289–1300.

(2) Helfrecht, B. A.; Cersonsky, R. K.; Fraux, G.; Ceriotti, M. Structure-property maps with Kernel principal covariates regression. *Machine Learning: Science and Technology* **2020**, *1*, 045021.

(3) Imbalzano, G.; Zhuang, Y.; Kapil, V.; Rossi, K.; Engel, E. A.; Grasselli, F.; Ceriotti, M. Uncertainty estimation for molecular dynamics and sampling. *The Journal of Chemical Physics* **2021**, *154*, 074102.

(4) Lamaka, S. V.; Vaghefinazari, B.; Mei, D.; Petrauskas, R. P.; Höche, D.; Zheludkevich, M. L. Comprehensive screening of Mg corrosion inhibitors. *Corrosion Science* **2017**, *128*, 224–240.